Electric Fields and Interference Effects inside Noncentrosymmetric Multilayer Films at Electrode Surfaces from Electrochemically Modulated Surface Plasmon Resonance Experiments

Dennis G. Hanken and Robert M. Corn*

Department of Chemistry, University of Wisconsin−Madison, 1101 University Avenue, Madison, Wisconsin 53706

The electric field profile inside a self-assembled noncentrosymmetric zirconium phosphonate (ZP) multilayer film at a gold electrode is determined by the in situ optical technique of electrochemically modulated surface plasmon resonance (EM-SPR). In these experiments, changes in the index of refraction (Δn) of a ZP film during potential modulation are measured via the EM-SPR differential reflectivity curves. Modulated SPR experiments on the ZP films incorporated into air-gap capacitors are used to relate Δn to changes in the electric field strength (ΔE) inside the film. The noncentrosymmetric ZP films utilize the nonlinear optical chromophores [5-[4-[[4-[(6-hydroxyhexyl)sulfonyl]phenyl]azo]phenyl]pentoxy]phosphonic acid (HAPA) and [1-[4-[4-[(N-(2-hydroxyethyl)-N-methyl)amino]phenyl]azo](5-phosphonopentyl)]pyridinium bromide (PY-AZO). For a 6.7 nm ZP HAPA film, a change in electrode potential ($\Delta\phi_m$) of 50 mV corresponds to a change in electric field strength (ΔE) of 1.4×10^4 V/cm. EM-SPR experiments on mixed ZP multilayers of HAPA and the centrosymmetric molecule 1,10-decanediylbis-(phosphonate) are used to measure the spatial variations of the electric fields within the ultrathin films. Evidence for ion and solvent penetration into the ZP films is observed in the electrochemical environment. Additional studies of interference effects in mixed multilayers of HAPA and PY-AZO are used to verify the retention of directional order during the ZP multilayer deposition process.

The strength of the electrostatic fields within the interfacial region of a chemically modified electrode is a fundamental parameter that controls the reactivity and electrochemistry of any chemical species incorporated into the thin film.[1−6] To date, there have been a limited number of studies that have determined field strengths within monolayer films at electrode surfaces,[7−12] and only a few measurements of the variations in the electric fields

as a function of position in the ultrathin film have been reported.[13−15] We have recently demonstrated that a novel extension of the surface plasmon resonance (SPR) technique, called electrochemically modulated surface plasmon resonance (EM-SPR), can be used to monitor electrostatic fields inside organic monolayer and multilayer films at electrode surfaces.[16] In this paper, we employ the EM-SPR technique to determine the electric field profile within self-assembled zirconium phosphonate (ZP) multilayers at electrode surfaces.

The EM-SPR method utilizes surface plasmons to measure the changes in the index of refraction of a noncentrosymmetric thin organic film that occur upon application of an external electrostatic field. Surface plasmons are surface electromagnetic waves whose wave vectors (k_{sp}) are parallel to the interface between a metal and a dielectric medium.[17,18] Surface plasmons can be created at a gold/electrolyte interface by the prism coupling of a HeNe laser ($\lambda = 632.8$ nm) to a thin (47 nm) gold film at a specific angle (θ_{sp}).[19] The wave vectors k_{sp} and, hence, θ_{sp} depend on the thickness and index of refraction of the dielectric medium in contact with the metal surface.[20,21] The EM-SPR experiment monitors the changes in a film's index of refraction that can occur upon modulation of the electrode potential.

This change in index of refraction (Δn) is referred to as the linear electrooptical effect, or Pockel's effect, and is the result of a nonlinear optical mixing process similar to second harmonic generation (SHG).[22] This effect requires a noncentrosymmetric thin film, and, in our experiments, we incorporate asymmetric nonlinear optical chromophores into ZP multilayers in order to obtain an EM-SPR response.[16,23−27] The two chromophores

(1) Bard, A. J.; Faulkner, L. R. *Electrochemical Methods*; J. Wiley: New York, 1980.

(2) Finklea, H. O. In *Electroanalytical Chemistry: A series of Advances*; Bard, A. J., Rubinstein, I., Eds.; Marcel Dekker, Inc.: New York, 1996; Vol. 19, pp 109.

(3) Smith, C. P.; White, H. S. *Anal. Chem.* **1992**, *64*, 2398.

(4) Smith, C. P.; White, H. S. *Langmuir* **1993**, *9*, 1.

(5) Fawcett, W. R.; Fedurco, M.; Kovacova, Z. *Langmuir* **1994**, *10*, 2403.

(6) Fawcett, W. R. *J. Electroanal. Chem.* **1994**, *378*, 117.

(7) Schmidt, P. H.; Plieth, W. J. *J. Electroanal. Chem.* **1986**, *201*, 163.

(8) Widrig, C. A.; Chung, C.; Porter, M. D. *J. Electroanal. Chem.* **1991**, *201*, 335.

(9) Pope, J. M.; Tan, Z.; Kimbrell, S.; Buttry, D. A. *J. Am. Chem. Soc.* **1992**, *114*, 10085.

(10) Pope, J. M.; Buttry, D. A. Private Communication.

(11) Lockhart, D. J.; Boxer, S. G. *Chem. Phys. Lett.* **1988**, *144*, 243.

(12) Lockhart, D. J.; Kirmaier, C.; Holten, D.; Boxer, S. G. *J. Phys. Chem.* **1990**, *94*, 6987.

(13) Creager, S. E.; Weber, K. *Langmuir* **1993**, *9*, 844.

(14) Rowe, G. K.; Creager, S. E. *J. Phys. Chem.* **1994**, *98*, 5500.

(15) Gao, X.; White, H. S.; Chen, S.; Abruna, H. D. *Langmuir* **1995**, *11*, 4554.

(16) Hanken, D. G.; Naujok, R. R.; Gray, J. M.; Corn, R. M. *Anal. Chem.* **1997**, *69*, 240.

(17) Burstein, E.; Chen, W. P.; Chen, Y. J.; Hartstein, A. *J. Vac. Sci. Technol.* **1974**, *11*, 1004.

(18) Raether, H. *Physics of Thin Films*; Academic: New York, 1977; Vol. 9, pp 145.

(19) Gordon, J. G.; Swalen, J. D. *Opt. Commun.* **1977**, *22*, 374−376.

(20) Swalen, J. D.; Gordon, J. G.; Philpott, M. R.; Brillante, A.; Pockrand, I.; Santo, R. *Am. J. Phys.* **1980**, *48*, 669.

(21) Pockrand, I.; Swalen, J. D.; Gordon, J. G.; Philpott, M. R. *Surf. Sci.* **1977**, *74*, 237.

(22) Shen, Y. R. *The Principles of Nonlinear Optics*; Wiley: New York, 1984.

utilized in this paper are depicted in Figure 1a, and are denoted as HAPA ([5-[4-[[4-[(6-hydroxyhexyl)sulfonyl]phenyl]azo]phenyl]-pentoxy]phosphonic acid) and PY-AZO ([1-[4-[4-[(N-(2-hydroxy-ethyl)-N-methyl)amino]phenyl]azo](5-phosphonopentyl)]pyridinium bromide). We have previously characterized the EM-SPR response of ZP films of these two chromophores;[16,27] an example of a noncentrosymmetric ZP film that incorporates a HAPA monolayer is depicted in Figure 1b.

In this paper, we examine mixed ZP films in which the overall film thickness, the number of chromophore layers, and the position of the nonlinear optical chromophores within the multilayer are varied. The EM-SPR technique is used to determine variations in the electric field strength within a series of mixed ZP multilayer films that contain monolayers of HAPA and the centrosymmetric molecule 1,10-decanediylbis(phosphonate) (DBP). Ion penetration into the films is found to decrease the electrostatic fields in the outer portions of the ZP multilayers. In an additional series of EM-SPR experiments, interference effects between the two nonlinear optical chromophores HAPA and PY-AZO inside a mixed ZP multilayer are used to show that directional order is preserved during the multilayer deposition process and that multiple types of oriented monolayers can be incorporated into a single ZP film.

EXPERIMENTAL CONSIDERATIONS

Materials. 2,4,6-Collidine (99%), phosphorus oxychloride (99%), zirconyl chloride octahydrate (98%), and dihexadecyl phosphate (DHP, 99%) were obtained from Aldrich Chemical Co. Other reactants and solvents included tetrabutylammonium bromide (99+%), sodium hydroxide (puriss), and o-phosphoric acid (puriss, Fluka), UV grade acetonitrile (Burdick and Jackson), and absolute ethanol (Pharmco). All chemicals were used as received. MUD (11-mercaptoundecanol), DBP (1,10-decanediylbis(phosphonate)), HAPA ([5-[4-[[4-[(6-hydroxyhexyl)sulfonyl]phenyl]azo]-phenyl]pentoxy]phosphonic acid) and PY-AZO ([1-[4-[4-[(N-(2-hydroxyethyl)-N-methyl)amino]phenyl]azo](5-phosphono-pentyl)]pyridinium bromide) were synthesized as described previously.[16,27,28] All aqueous solutions were prepared from 18 MΩ Millipore-filtered water.

Polarization−Modulation Fourier Transform Infrared Reflection Absorption Spectroscopy (PM-FTIRRAS) Measurements on Gold Substrates. All PM-FTIRRAS spectra were obtained on a Mattson RS-1 spectrometer without a background or reference spectrum utilizing real-time interferogram sampling electronics that have been described previously.[29,30] The differential reflectance (%$\Delta R/R$) spectra were converted to absorbance units for comparison with other spectra. Sample spectra in the mid-infrared region (1800−850 cm^{-1}) were obtained with a narrow-band HgCdTe detector. All infrared spectra were acquired at 2 cm^{-1} resolution from 1024 interferometer scans.

SPR and Electrooptical Measurements on Gold Substrates. The experimental apparatus for scanning and electro-

(23) Putvinski, T. M.; Schilling, M. L.; Katz, H. E.; Chidsey, C. E. D.; Mujsce, A. M.; Emerson, A. B. *Langmuir* **1990**, *6*, 1567.
(24) Katz, H. E.; Scheller, G.; Putvinski, T. M.; Schilling, M. L.; Wilson, W. L.; Chidsey, C. E. D. *Science* **1991**, *254*, 1485.
(25) Katz, H. E. *Chem. Mater.* **1994**, *6*, 2227.
(26) Katz, H. E.; Wilson, W. L.; Scheller, G. *J. Am. Chem. Soc.* **1994**, *116*, 6636.
(27) Hanken, D. G.; Corn, R. M. *Isr. J. Chem.*, in press.
(28) Frey, B. L.; Hanken, D. G.; Corn, R. M. *Langmuir* **1993**, *9*, 1815.
(29) Green, M. J.; Barner, B. J.; Corn, R. M. *Rev. Sci. Instrum.* **1991**, *62*, 1426.
(30) Barner, B. J.; Green, M. J.; Saez, E. I.; Corn, R. M. *Anal. Chem.* **1991**, *63*, 55.
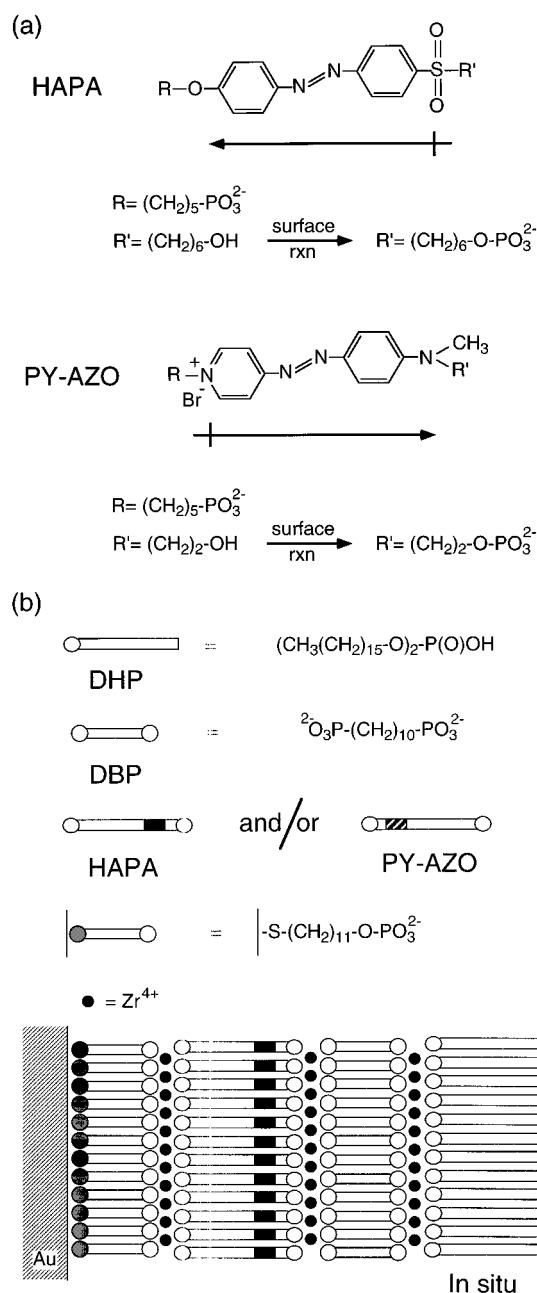
Figure 1. (a) Structures and associated dipole moments (black arrows) for the nonlinear optical chromophores HAPA ([5-[4-[[4-[(6-hydroxyhexyl)sulfonyl]phenyl]azo]phenyl]pentoxy]phosphonic acid) and PY-AZO ([1-[4-[4-[(N-(2-hydroxyethyl)-N-methyl)amino]phenyl]-azo](5-phosphonopentyl))]pyridinium bromide) used in these experiments to form noncentrosymmetric zirconium phosphonate (ZP) multilayer films on gold surfaces. (b) Schematic diagram for the construction of noncentrosymmetric mixed zirconium phosphonate multilayer films. The ZP films are created on vapor-deposited gold substrates that have been primed with a self-assembled monolayer of phosphorylated MUD (11-mercaptoundecanol). Exposure of the zirconated surface to solutions of the nonlinear optical compounds HAPA and/or PY-AZO following the procedure of Katz and co-workers led to noncentrosymmetric multilayer films. For electric field profile experiments, N DBP (1,10-decanediylbis(phosphonate)) layers, where N = 0−8, are self-assembled onto the HAPA monolayer (see text). The films were then capped with a self-assembled monolayer of DHP (dihexadecyl phosphate) and characterized in an electrochemical environment with EM-SPR.

chemically modulated surface plasmon resonance measurements is shown in Figure 2. This apparatus measured the reflectivity of p-polarized light from a HeNe laser (632.8 nm, 1 mW, Newport
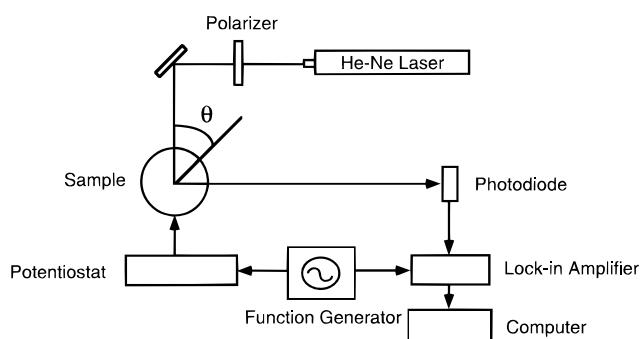
In Situ SP Modulation Experiment

Figure 2. Experimental apparatus for EM-SPR measurements. The apparatus measures the reflectivity (%R) and differential reflectivity (Δ%R) of p-polarized light at 632.8 nm (HeNe laser) from the SF-10/Au/ZP film/electrolyte interface as a function of incident angle, θ, in an electrochemical environment. For scanning SPR measurements, the reflectivity (%R vs θ) was measured at a fixed electrode potential (0.0 V vs SCE). For EM-SPR measurements, the differential reflectivity (Δ%R vs θ) due to the electrooptical (Pockel's) effect was measured by modulating the electrode potential about a fixed potential ($\Delta\phi_m$= 50−760 mV, at 1 kHz, at 0.0 V vs SCE).

Corp.) from the SF-10/Au/ZP film sample as a function of the incident angle, θ. The ZP-coated thin gold samples (47 nm) formed on SF-10 glass slides (Schott) were placed in optical contact with an SF-10 equilateral prism (Ealing Electro-Optics, Inc.) using an index matching fluid (1-iodonaphthalene, Aldrich). The sample cell shown in the insets of Figures 4 and 8 consisted of a Teflon electrochemical cell that was pressed against the ZP-coated thin gold sample by use of a Viton O-ring for a water-tight seal. A three-electrode assembly was formed with the ZP-coated gold sample as the working electrode, a saturated calomel reference electrode, and a platinum counter electrode. The potential was controlled by a potentiostat (EG&G Model 173 potentiostat/galvanostat) and a voltage controller (EG&G Model 175 universal programmer). All in situ electrochemical experiments were carried out using nitrogen-purged 0.2 M tetrabutylammonium bromide as the electrolyte. Cyclic voltammograms were recorded in the potential region from −0.4 to 0.6 V vs SCE. For the EM-SPR experiments, the potential was fixed to 0.0 V vs SCE, and a small sinusoidal modulation ($\Delta\phi_m$= 50−760 mV, 1 kHz, Model 5100B function generator, Krohn&Hite) was applied to the electrochemical cell. This modulation produced a corresponding modulation in the reflectivity which was detected by a photodiode (Hamamatsu) and a lock-in amplifier (SR510, Stanford Research Systems). For regular scanning SPR measurements, the potential was fixed to 0.0 V vs SCE, and no modulation voltage was applied. Air-gap electrooptical experiments on the HAPA and PY-AZO films (not shown) were performed as described previously.[16] The changes in index of refraction Δn for the ZP HAPA multilayer films were determined from Fresnel fits to the EM-SPR differential reflectivity curves by subtracting two surface plasmon theory curves which differed by small changes in the real component of the dielectric constant of the ZP film. These theoretical Fresnel calculations were performed using a N-phase model, where N = 5−9, and have been described in detail elsewhere.[16,27,31−33]

(31) Jordan, C. E.; Frey, B. L.; Kornguth, S.; Corn, R. M. *Langmuir* **1994**, *10*, 3642.
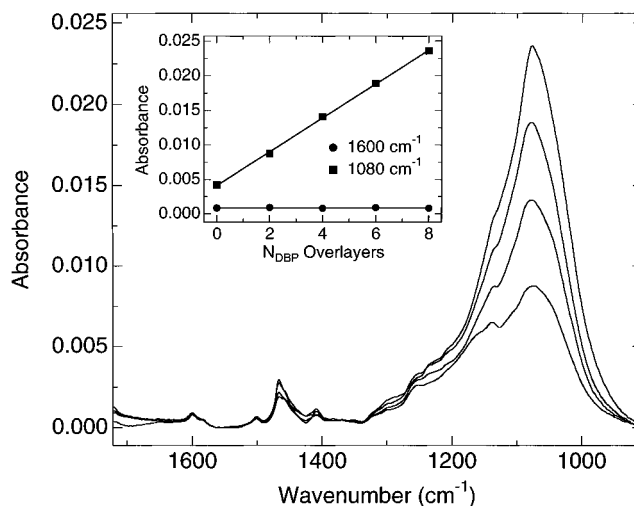
Figure 3. Mid-infrared region of the PM-FTIRRAS spectrum for a series of mixed ZP multilayer films that consisted of a phosphorylated MUD primer layer, one HAPA monolayer, N DBP monolayers, where N varied from 0 to 8, and one DHP capping monolayer. These spectra contain vibrational bands due to both HAPA and DBP monolayers. The inset graph plots the absorbances of two of these bands (1600 and 1080 cm⁻¹) as a function of increasing DBP overlayers. The intensity of the 1600 cm⁻¹ band, which has been previously attributed to the HAPA aromatic ring stretch, remains constant with increasing DBP overlayers. The intensity of the 1080 cm⁻¹ phosphate/phosphonate band of the ZP HAPA and ZP DBP layers increases in a linear fashion with the same slope as that measured for pure ZP DBP films.

RESULTS AND DISCUSSION

A. Spectroscopic Characterization of Mixed ZP Multilayer Films.

Mixed noncentrosymmetric ZP multilayer films incorporating the nonlinear optical chromophores HAPA and PY-AZO and the centrosymmetric molecule DBP were characterized with a combination of polarization−modulation Fourier transform infrared reflection−absorption spectroscopy (PM-FTIRRAS) for molecular structure information and surface plasmon resonance (SPR) measurements for the optical determination of film thickness prior to all EM-SPR experiments. We have effectively used this combination of techniques in the past to verify the formation of various biological and ZP multilayer films on gold surfaces.[16,27,28,31−34] In this section, the characterization of three sets of mixed ZP multilayer films are detailed, two incorporating HAPA and DBP layers and the third incorporating HAPA and PY-AZO layers. These mixed ZP films were formed on vapor-deposited gold surfaces using a phosphorylated MUD primer monolayer. In addition, these ZP films were terminated with a self-assembled monolayer of DHP. This capping monolayer produced very hydrophobic gold electrode surfaces that should reduce electrolyte penetration into the film.

First, the mid-infrared region of the PM-FTIRRAS spectrum for a series of mixed ZP multilayer films that consisted of a phosphorylated MUD primer layer, one HAPA monolayer, N DBP monolayers, where N varied from 0 to 8, and one DHP capping monolayer are shown in Figure 3. These spectra contain vibrational bands due to both HAPA and DBP monolayers. The inset graph in Figure 3 monitors the absorbances of two of these bands (1600 and 1080 cm⁻¹) as a function of increasing DBP

(32) Hanken, D. G.; Corn, R. M. *Anal. Chem.* **1995**, *67*, 3767.

(33) Frey, B. L.; Jordan, C. E.; Kornguth, S.; Corn, R. M. *Anal. Chem.* **1995**, *67*, 4452.

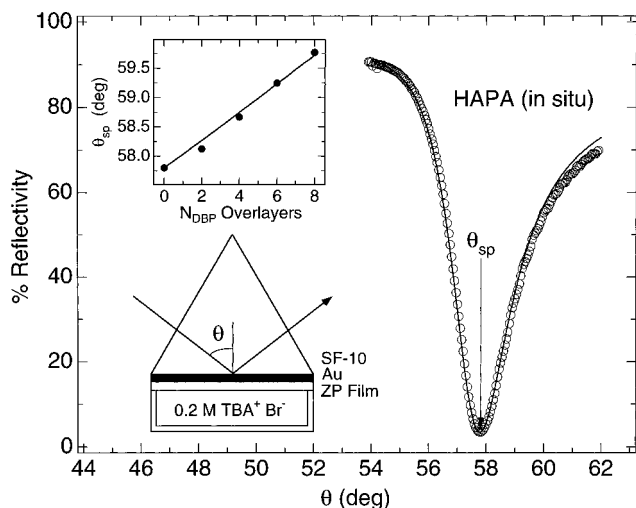(34) Frey, B. L.; Corn, R. M. *Anal. Chem.* **1996**, *68*, 3193.

Figure 4. In situ scanning SPR reflectivity curve obtained for a ZP film that consisted of a phosphorylated MUD primer layer, one HAPA monolayer, and one DHP capping monolayer on a gold substrate (open circles). The curve is the measured reflectivity (%R) of p-polarized light at 632.8 nm from the SF-10/Au/ZP film/electrolyte interface as a function of incident angle, θ. The minimum in the measured reflectivity corresponds to the coupling of the incident laser light with surface plasmons at the Au/ZP film/electrolyte interface. The angle at which this minimum occurs is called the surface plasmon angle, θ_{sp}. The solid line in the figure is a five-phase Fresnel fit to the SPR data (see text). The inset graph follows the shift in θ_{sp} upon the formation of N DBP monolayers, where N varied from 0 to 8. The solid line in the inset graph is a seven-phase Fresnel fit to the data and yields the average ZP film thickness (see text).

Figure 5. Mid-infrared region of the PM-FTIRRAS spectrum for a series of mixed ZP multilayer films that consisted of a phosphorylated MUD primer layer, one HAPA monolayer, six DBP monolayers, and one DHP capping monolayer (1 HAPA + 6 DBP ZP film). In these films, the position of the HAPA layer is systematically varied within the multilayer. The inset graph monitors the intensities of three different vibrational bands (1600, 1466, and 1080 cm^{-1}) as a function of the HAPA layer position within the multilayer. As the HAPA layer position is varied within the ZP film, the measured intensities for the different bands remain constant to within 10%.

overlayers. The intensity of the 1600 cm^{-1} band, which has been previously attributed to the HAPA aromatic ring stretch, remains constant with increasing DBP overlayers as expected, while the intensity of the 1080 cm^{-1} phosphate/phosphonate band of the ZP HAPA and ZP DBP layers increases in a linear fashion.[16] The slope of this line is the same as that previously measured for ZP DBP multilayer films.[28,32] The linear increase in the intensity of this band indicates that each subsequent DBP monolayer has an equivalent molecular structure and packing density.

In order to measure the thickness of the ZP films, in situ scanning SPR measurements were also performed on mixed ZP multilayers of HAPA and DBP. In these measurements (pictured in Figure 4), the reflectivity (%R) of a p-polarized HeNe laser is monitored as a function of the incident angle (θ) for a prism/gold/ZP film/electrolyte interface. The ZP film in this experiment consisted of a phosphorylated MUD primer monolayer, one HAPA ZP monolayer, and one DHP capping layer (see Figure 1b). As the angle of incidence is varied, just beyond the critical angle the reflectivity sharply decreases to a minimum point designated as the surface plasmon angle, θ_{sp}. At this angle, the laser light is coupled into surface plasmon modes at the gold/ZP film/electrolyte interface. The angle θ_{sp} changes as additional multilayers are deposited onto the gold surface, and this shift in θ_{sp} can provide a quantitative measure of the ZP film thickness (d) if the film index of refraction (n) is known.[19-21,31-33] The solid line in Figure 4 is a five-phase Fresnel calculation using values of n described previously and an overall thickness d of 6.7 nm as determined from ex situ scanning SPR measurements.[16] The inset graph in Figure 4 follows the angular shift in θ_{sp} with increasing DBP overlayers relative to the HAPA monolayer film. The solid line is a seven-phase Fresnel fit to the data again using values of
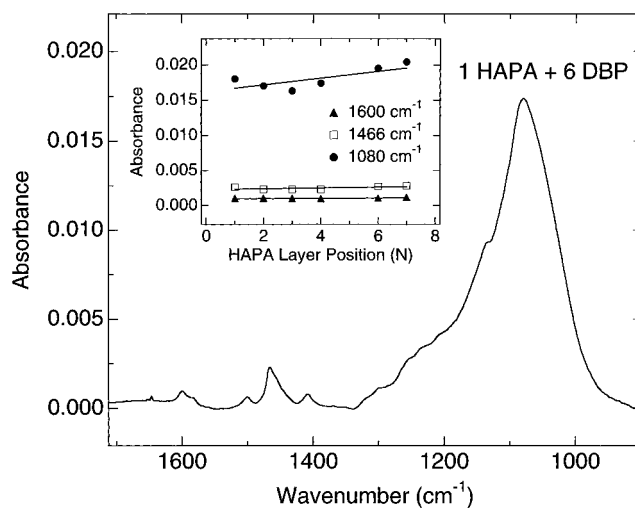
n determined previously and corresponds to an increase in the ZP film thickness of 1.6 ± 0.2 nm per DBP monolayer. This DBP layer spacing is equivalent to that measured ex situ for multilayer DBP films. These results indicate that stable, reproducible mixed multilayers of HAPA and DBP are formed on the gold electrode surface.

PM-FTIRRAS and in situ SPR are also used to examine mixed ZP films in which the position of a single HAPA monolayer is systematically varied in a fixed multilayer DBP film. Figure 5 shows the mid-infrared region for a ZP film that consisted of a phosphorylated MUD primer layer, one HAPA monolayer, six DBP monolayers, and one DHP capping monolayer (this multilayer is referred to as the 1 HAPA + 6 DBP ZP film). This spectrum is equivalent to that observed for the similar ZP film in Figure 3. The inset graph in Figure 5 monitors the intensities of three different vibrational bands (1600, 1466, and 1080 cm^{-1}) as a function of the HAPA layer position within the multilayer. As the HAPA layer is varied within the ZP film, the measured intensities for the different bands remain constant to within 10%. This again indicates that, during the ZP film deposition process, the structure and packing density of both the HAPA and DBP portions of the film are maintained regardless of the HAPA layer position. SPR measurements (not shown) also support this conclusion, in that the average total thicknesses for the various 1 HAPA + 6 DBP films all agree to within 8% (17 ± 1 nm).

For mixed noncentrosymmetric ZP films incorporating the two different NLO chromophores HAPA and PY-AZO, the PM-FTIRRAS technique is useful in determining whether the retention of monolayer structure is maintained upon self-assembly of multilayers with different dipole moments. As detailed in section D, a series of samples were constructed with varying numbers of PY-AZO and HAPA monolayers. Figure 6 shows the mid-infrared spectrum for a mixed ZP film that consisted of a phosphorylated MUD primer layer, two PY-AZO monolayers, one HAPA monolayer, and one DHP capping monolayer (2 PY-AZO + 1 HAPA ZP
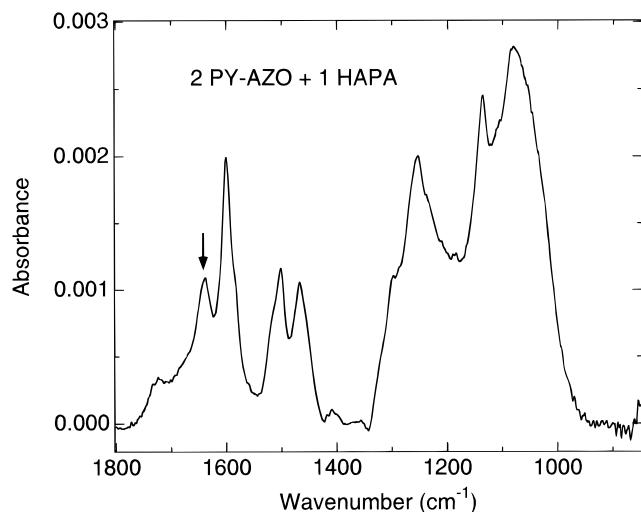
Figure 6. Mid-infrared spectrum for a mixed ZP film that consisted of a phosphorylated MUD primer layer, two PY-AZO monolayers, one HAPA monolayer, and one DHP capping monolayer (2 PY-AZO + 1 HAPA ZP film). This spectrum contains vibrational bands due to both HAPA and PY-AZO monolayers, with the band at 1639 cm^{-1} (labeled with the black arrow) being solely due to the PY-AZO pyridinium functionality.

film). This spectrum contains vibrational bands due to both HAPA and PY-AZO monolayers, with the band at 1639 cm^{-1} (labeled with the black arrow) being solely due to the PY-AZO pyridinium functionality. The retention of monolayer structure within these mixed ZP films is monitored by comparing the intensities of the 1600, 1501, and 1254 cm^{-1} bands to those from pure PY-AZO and HAPA film spectra obtained previously.[16,27] For the different ZP films examined in section D, the measured band intensities all agree to within 10% of the intensities expected from calculations using the spectra of pure ZP PY-AZO and HAPA films. These results suggest that the HAPA and PY-AZO layers maintain their structural order during the ZP film deposition process and do not mix.

B. EM-SPR Experiments and Measurements of Electric Field Strengths inside Multilayer Films on Electrode Surfaces. The EM-SPR experiment measures the change in reflectivity ($\Delta\%R$) that occurs upon potential modulation ($\Delta\phi_m$) as a function of incident angle θ. These experimental EM-SPR differential reflectivity curves can be modeled with complex Fresnel calculations in order to relate the measured $\Delta\%R$ to the change in the film's index of refraction, Δn.[35-37] An example of how Fresnel calculations can be used to relate $\Delta\%R$ and Δn is depicted in Figure 7. Figure 7a plots two surface plasmon theory curves for two thin films that differ in index of refraction. The difference between these two curves produces the differential reflectivity curve shown in Figure 7b. This theoretical $\Delta\%R$ curve is used to fit the experimental EM-SPR data and results in the determination of Δn for a given $\Delta\phi_m$. From this Δn value, the change in electric field strength (ΔE) within the film due to potential modulation at a charged electrode can be determined by eq 1,[37] where n is the optical index of refraction of the film, which is determined by

(35) Cross, G. H.; Girling, I. R.; Peterson, I. R.; Cade, N. A.; Earls, J. D. *Electron. Lett.* **1986**, *22*, 1111.
(36) Cross, G. H.; Girling, I. R.; Peterson, I. R.; Cade, N. A.; Earls, J. D. *J. Opt. Soc. Am. B* **1987**, *4*, 962.
(37) Sekkat, Z.; Kang, C.-S.; Aust, E. F.; Wegner, G.; Knoll, W. *Chem. Mater.* **1995**, *7*, 142.
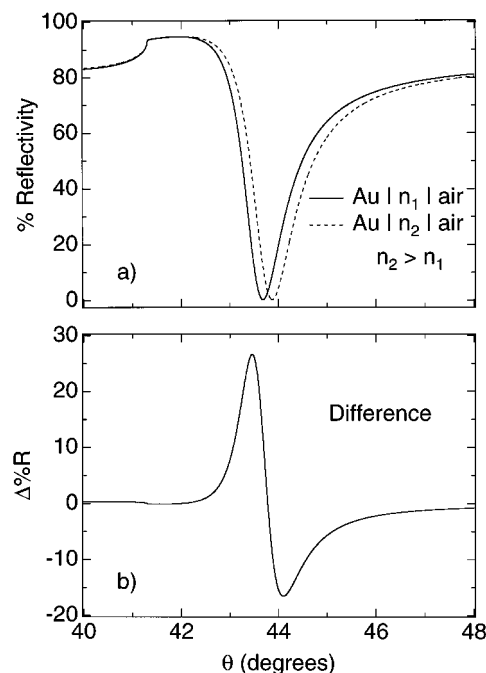
Figure 7. Method for modeling the measured EM-SPR differential reflectivity curves. (a) Two surface plasmon curves generated from Fresnel calculations which differ in the film's index of refraction. (b) The differential reflectivity curve produced from the difference between the two curves in (a). This theoretical $\Delta\%R$ curve is used to fit the experimental EM-SPR data and results in the determination of Δn for a given $\Delta\phi_m$. From this Δn value, the change in electric field strength (ΔE) within the film due to potential modulation at a charged electrode can be determined (see text).

$$\Delta E = 2\Delta n / n^3 r_{33} \tag{1}$$

ellipsometric experiments on thick ZP multilayer films,[16,32] and r_{33} is the electrooptic coefficient for the noncentrosymmetric ZP film, which is obtained from modulated SPR measurements on air-gap capacitors.[35,36] We have previously determined the magnitude of r_{33} for both HAPA and PY-AZO ZP monolayers to be 11 and -8 pm/V, respectively, at a wavelength of 632.8 nm.[16,27] Using these values of r_{33}, EM-SPR experiments can be used to monitor the changes in electric field strength (ΔE) that occur within a noncentrosymmetric multilayer film during the modulation of the electrode potential ($\Delta\phi_m$) in an electrochemical environment.

A schematic diagram of the electrochemical cell used in the EM-SPR experiments is shown in the inset of Figure 8. The electrochemical cell consisted of a Teflon cell that is pressed against the modified gold electrode with an O-ring seal. A three-electrode potentiostat with the thin gold film as the working electrode is used to control the potential and interfacial electric fields. A cyclic voltammogram (CV) of a gold electrode coated with a 1 HAPA + 4 DBP ZP film of thickness 13 ± 1 nm is shown in Figure 8; the CV shows no faradaic processes over a wide potential range from -0.4 to 0.6 V vs SCE. For the EM-SPR experiments, the electrode potential was set to 0.0 V vs SCE, and a sinusoidal waveform was applied ($\Delta\phi_m = 50-760$ mV at 1 kHz) to the electrochemical system. No changes in the measured EM-SPR response were observed for modulation frequencies from 0.2 to 1.5 kHz. The differential reflectivity ($\Delta\%R$) was then measured as a function of the incident angle. These differential reflectivity curves were used to obtain Δn, which in turn were converted to ΔE values using the previously determined r_{33} value for HAPA and eq 1.
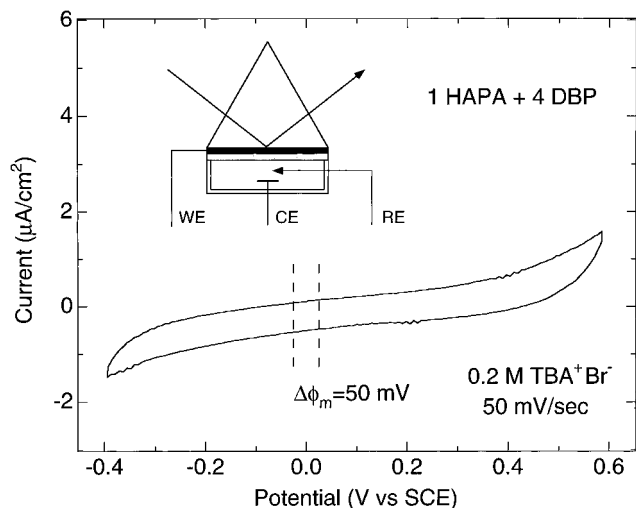
Figure 8. Cyclic voltammogram for a 13 ± 1 nm thick ZP multilayer film that consisted of a phosphorylated MUD primer layer, one HAPA monolayer, four DBP monolayers, and one DHP capping monolayer on a vapor-deposited gold substrate. This sample is referred to as the 1 HAPA + 4 DBP ZP film. A three-electrode assembly was formed, with the ZP-coated Au film as the working electrode, a saturated calomel reference electrode, and a platinum counter electrode. The CV was obtained in the region from -0.4 to 0.6 V vs SCE in 0.2 M tetrabutylammonium bromide at a scan rate of 50 mV/ s. For EM-SPR, the electrode potential was fixed to 0.0 V vs SCE, and a small sinusoidal modulation ($\Delta\phi_m = 50-760$ mV, at 1 kHz) was applied to the cell.
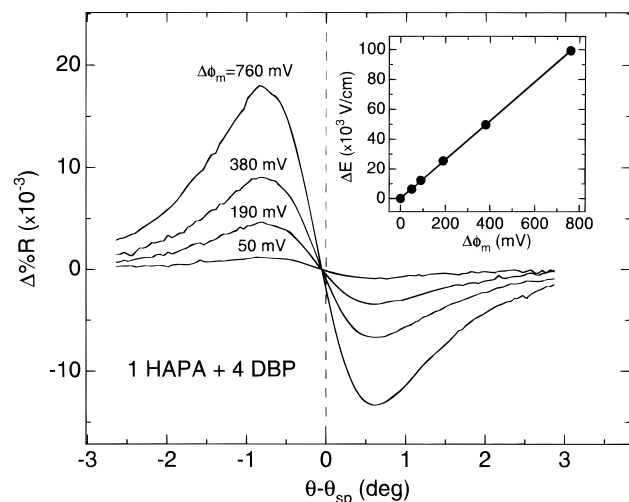

Figure 9. Differential reflectivity ($\Delta\%R$) obtained by EM-SPR measurements in 0.2 M tetrabutylammonium bromide for the 1 HAPA + 4 DBP ZP film. The curves are the overlay of increasing electrode modulation potentials ($\Delta\phi_m$) of 50, 190, 380, 760 mV about 0.0 V vs SCE, at 1 kHz, respectively. The differential reflectivities ($\Delta\%R$) measured in situ are converted to a change in electric field strength (ΔE) within the self-assembled multilayer film by comparison to air-gap electrooptical experiments (see text). The changes in the electric field strengths within the multilayer ZP film shown in the inset graph are surprisingly linear, with the applied modulation potential in the experimentally measured electrochemical potential window from -0.4 to 0.6 V vs SCE.

Figure 9 plots the differential reflectivity curves observed from a 1 HAPA + 4 DBP multilayer for a series of different modulation potentials. The x-axis in this figure is the difference between the incident angle and the surface plasmon angle ($\theta - \theta_{sp}$). The shape of the $\Delta\%R$ curves does not change with increasing modulation voltage and is similar to that reported previously for a HAPA

monolayer.[16] This waveform is predicted from Fresnel calculations for a positive Δn, as shown in Figure 7. In addition, the Fresnel calculations predict a zero-crossing point of $\theta - \theta_{sp} = -0.06°$ for all of the $\Delta\%R$ curves; this prediction agrees with the experimental data in the figure. From these Fresnel calculations, values for Δn are obtained and range from $\Delta n = 1.6 \times 10^{-5}$ for $\Delta\phi_m = 50$ mV to $\Delta n = 2.4 \times 10^{-4}$ for $\Delta\phi_m = 760$ mV.

As mentioned above, the experimentally determined Δn can be related to the change in electric field strength (ΔE) within the multilayer film at the electrode surface using the HAPA r_{33} value obtained from air-gap experiments. The ΔE values obtained from eq 1 for different modulation potentials in the 1 HAPA + 4 DBP sample are shown in the inset graph of Figure 9. The change in field strength is found to be surprisingly linear for applied modulation potentials from 0 to 760 mV and corresponds to a ΔE of 6.5×10^3 V/cm for a $\Delta\phi_m$ of 50 mV (1.3×10^5 V/cm per volt modulation). This value for ΔE within the 13 ± 1 nm multilayer ZP film is consistent with the field strength determined by Pope and Buttry inside a monolayer film at a silver electrode from fluorescent shift measurements.[9,10]

C. Electric Field Profile Measurements inside Multilayer Films. In a series of experiments on mixed HAPA/DBP multilayers, EM-SPR measurements were used to map out the electric field profile within ultrathin films at electrode surfaces. In these experiments, a single HAPA monolayer was used to probe the electric field at a specific point within the ZP film. A first set of EM-SPR experiments was performed on a series of five HAPA/ DBP monolayers that consisted of a phosphorylated MUD primer monolayer, one HAPA monolayer, N DBP monolayers, where N varied from 0 to 8, and a DHP capping monolayer. In each of these films, the HAPA monolayer was the first ZP monolayer deposited onto the electrode surface. The mixed multilayer films were characterized prior to the EM-SPR experiments with PM-FTIRRAS and scanning in situ SPR measurements (see section A). These measurements indicate that the thicknesses of the ZP films increase by 1.6 ± 0.2 nm per DBP monolayer (total film thicknesses from $6.7-20$ nm for $0-8$ DBP overlayers), with no observable changes in HAPA film structure and packing density. This DBP monolayer thickness is equivalent to that measured previously ex situ for multilayer DBP films.[32] These results indicate that stable, reproducible mixed multilayers of HAPA and DBP are formed on the gold electrode surface. The change in electric field strength at the HAPA monolayer position for a $\Delta\phi_m$ of 50 mV was determined from EM-SPR differential reflectivity measurements on each of the films as detailed in section B; the results of these experiments are plotted in Figure 10. A decrease in ΔE of up to 65% is observed as the number of centrosymmetric DBP monolayers is increased.

This decrease in the measured EM-SPR signal is attributed to the increase in overall thickness (d) of the ZP film due to the formation of DBP overlayers and has the functional form of $1/d$. A simple Helmholtz model of the electrochemical double-layer also predicts that the electric field strength should decrease with film thickness as $1/d$, assuming a fixed static dielectric constant ϵ.[1] (Please note that the ΔE values reported in this paper do not depend on the Helmholtz model of the double layer; they are determined directly from the optical measurements via eq 1.) For pure ZP films of DBP and HAPA-like chromophores, the static dielectric constants have been determined previously to be 4 and 7, respectively.[38,39] The solid line in Figure 10 is a theoretical curve
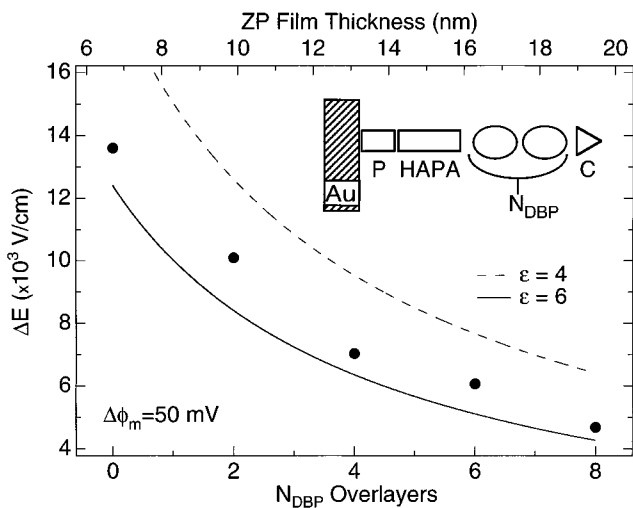
Figure 10. Change in electric field strength (ΔE) within a noncentrosymmetric ZP/HAPA film for increasing numbers of DBP overlayers ($N_{DBP} = 0-8$). The ΔE values are determined via the EM-SPR differential reflectivity curves for a HAPA monolayer whose position was fixed in the film (see inset). The positions labeled P and C in the inset correspond to the phosphorylated MUD primer layer and the DHP capping monolayer, respectively. The solid and dashed lines are fits to the experimental data using a simple Helmholtz model and ZP film thicknesses of 6.7–20 nm as determined from both in situ and ex situ SPR measurements (see text).

Figure 11. Variation in the change in electric field strength (ΔE) within a 17 ± 1 nm thick multilayer ZP film that consisted of a phosphorylated MUD primer monolayer, one HAPA monolayer, six DBP monolayers, and one DHP capping monolayer. These ΔE values are obtained via changes in the EM-SPR reflectivity curves by systematically varying the position of the HAPA monolayer within the multilayer ZP film (see inset). The linear decrease in ΔE is attributed to ion and solvent penetration into the multilayer film and implies a quadratic decrease with thickness of the local potential ϕ inside the ZP film (see text).

generated from the Helmholtz model using the ZP film thicknesses determined from in situ and ex situ SPR measurements (total film thicknesses vary from 6.7 to 20 nm for 0–8 DBP overlayers) and a static dielectric constant of 6. The dashed line in the figure is the same theoretical curve, but using a value of 4 for ϵ. Although the experimentally determined ΔE values parallel the Helmholtz model using an ϵ of 6, the effective dielectric constant for these mixed ZP films should vary from 6 to 4 as more DBP overlayers are assembled.

Deviations from a simple Helmholtz picture for the measured ΔE values inside the ZP multilayers are even more apparent in a second set of experiments. In these measurements, a series of mixed HAPA/DBP films were prepared in which the total thickness was held constant and the position of the HAPA monolayer was varied. These films consisted of a phosphorylated MUD primer layer, one HAPA monolayer, six DBP monolayers, and a DHP capping monolayer (1 HAPA + 6 DBP ZP films). As depicted in Figure 11, the position of the HAPA monolayer was varied from closest to the electrode surface ($N = 1$) to farthest away from the surface ($N = 7$). These mixed ZP films were characterized prior to the EM-SPR experiments with PM-FTIRRAS and scanning in situ SPR measurements (see section A); no significant changes in film structure, molecular orientation, or overall film thickness (17 ± 1 nm) were observed as the HAPA monolayer position was varied. Figure 11 plots the change in the electric field strength (ΔE) for a potential modulation $\Delta\phi_m$ of 50 mV as a function of the position of HAPA in a sample (N). These ΔE values were again obtained from the experimentally measured EM-SPR differential reflectivity curves. As the HAPA layer is placed farther away from the electrode surface, a linear decrease in ΔE is observed, with a maximum loss of 50% at the outermost
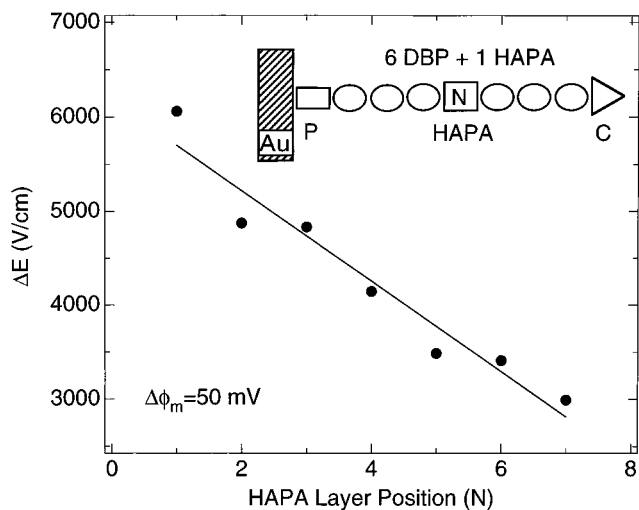
($N = 7$) position. This decrease is not expected from a simple parallel plate capacitor model of the interface, which would predict a constant electric field inside the film.[1]

A number of possibilities exist to account for the observed decrease in ΔE: (i) the orientation or tilt angle of the HAPA chromophores is changing with position in the multilayer film; (ii) changes in the HAPA layer packing density as a function of position in the mixed ZP films are taking place; (iii) noncentrosymmetry is lost in the ZP film due to HAPA intercalation and randomization into the DBP portions of the multilayer; or (iv) ion and solvent penetration occurs into the ZP multilayer, resulting in a decrease in the electric field strength within the film. The PM-FTIRRAS and in situ SPR characterization measurements made on these mixed ZP films as discussed in section A eliminate the first three possible sources of the measured decrease in ΔE; all of the data show that, during the ZP film deposition process, no significant changes in film uniformity, packing density, molecular orientation, or overall film thickness take place for the various multilayer films. This suggests that the experimentally measured linear decrease in ΔE is a result of ion and solvent penetration into the ZP film in the electrochemical environment. A linear decrease in ΔE implies a quadratic decrease with thickness of the local potential ϕ inside the ZP film; i.e., redox species incorporated into this ZP film at the $N = 7$ position would experience only 25% of the applied potential ϕ_m. The effect of the local potential on the electrochemical response of ultrathin organic films at electrode surfaces has been discussed previously,[2–6,8,40,41] and the EM-SPR measurements described in this paper provide a method for quantitation of the local electrostatic potential within these films.

D. EM-SPR Interference Effects within Mixed HAPA/PY-AZO Multilayer Films. In a final set of EM-SPR experiments,

(38) Kepley, L. J.; Sackett, D. D.; Bell, C. M.; Mallouk, T. E. *Thin Solid Films* **1992**, 132.
(39) Katz, H. E.; Schilling, M. L. *Chem. Mater.* **1993**, *5*, 1162.

(40) Evans, S. D.; Ulman, A. *Chem. Phys. Lett.* **1990**, 170, 462.
(41) Becka, A. M.; Miller, C. J. *J. Phys. Chem.* **1993**, *97*, 6233.

we used interference effects between two different noncentrosymmetric ZP monolayers to establish the relative directional order in mixed multilayers at electrode surfaces. In addition to the HAPA chromophore, we have characterized the EM-SPR response of ZP multilayers of a second nonlinear optical chromophore, PY-AZO, which is pictured in Figure 1a. The dipole moment of the PY-AZO molecule points in the opposite direction of the HAPA molecule; i.e., in PY-AZO, the dipole moment points away from the phosphonate group as compared to the dipole moment in HAPA, which points toward the phosphonate end of the molecule (see Figure 1a). When assembled into a ZP film at an electrode surface, this chromophore exhibited an EM-SPR response that we have reported previously.[27] The electrooptic coefficient r_{33} for a PY-AZO monolayer is -8 pm/V; this value of r_{33} has the opposite sign and is slightly smaller than r_{33} for a HAPA monolayer ($+11$ pm/V).

The fact that r_{33} has opposite signs for HAPA and PY-AZO monolayers is reflected in the shape of the EM-SPR differential reflectivity curves for the two ZP films. As shown in Figure 9, the $\Delta\%R$ curve for HAPA has a maximum at an angle below θ_{sp} ($\theta - \theta_{sp} < 0$) and a minimum above θ_{sp} ($\theta - \theta_{sp} > 0$). In contrast, $\Delta\%R$ curves for PY-AZO films are found to exhibit the opposite shape, i.e., a maximum at an angle above θ_{sp} and a minimum below θ_{sp}. This difference is predicted by the Fresnel calculations and is due to the fact that Δn is opposite in sign for the HAPA and PY-AZO films.

The electrooptical response r from the interface can also be described as the complex surface nonlinear susceptibility $\chi^{(2)}(-\omega,\omega,)$.[37,42-44] In addition to a magnitude, $\chi^{(2)}(-\omega,\omega,0)$ also has a phase component associated with it. The phase of $\chi^{(2)}$ has been used previously in SHG experiments to ascertain the absolute orientation of a monolayer film.[45] For example, interference effects have been observed in the SHG from mixed monolayers of two similar chromophores pointing in opposite directions at a liquid/liquid interface.[46] This same type of cancellation effect should also be possible in EM-SPR experiments on mixed ZP films containing both HAPA and PY-AZO monolayers.

To demonstrate this effect, EM-SPR measurements were performed on a set of three mixed HAPA/PY-AZO multilayer films: (i) a ZP film with two PY-AZO monolayers and one HAPA monolayer, (ii) a ZP film with one PY-AZO monolayer and two HAPA monolayers, and (iii) a ZP film with one PY-AZO and one HAPA monolayer. Each of these ZP multilayers contained a phosphorylated MUD primer layer and a DHP capping monolayer. As discussed in section A, each of these ZP films was characterized with PM-FTIRRAS prior to the EM-SPR measurements. The PM-FTIRRAS spectra indicate that the mixed HAPA and PY-AZO films form layers with molecular structures and packing densities that are equivalent to those observed for pure films of the two chromophores. The EM-SPR differential reflectivity curves for these three films are shown in Figures 12 and 13. The $\Delta\%R$ curve for the 1 PY-AZO + 2 HAPA ZP film in Figure 12a has a waveform similar to the $\Delta\%R$ curve for a single HAPA monolayer, whereas the $\Delta\%R$ curve for the 2 PY-AZO + 1 HAPA sample in Figure 12b
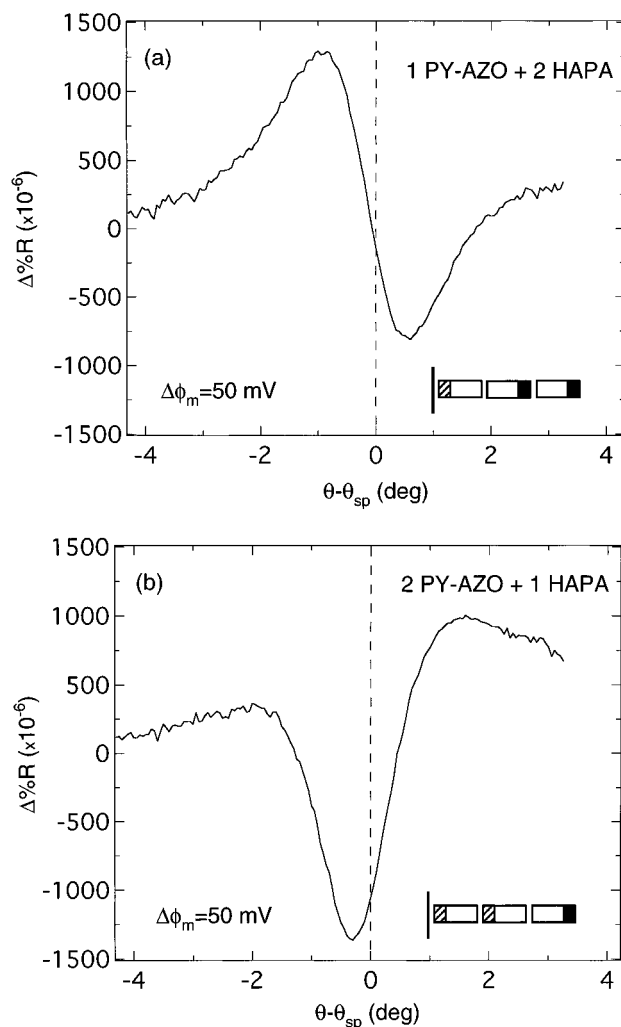
(42) Singer, K. D.; Kuzyk, M. G.; Sohn, J. E. *J. Opt. Soc. Am. B* **1987**, *4*, 968.
(43) Robello, D. R.; Dao, P. T.; Phelan, J.; Revelli, J.; Schildkraut, J. S.; Scozzafava, M.; Ulman, A.; Willand, C. S. *Chem. Mater.* **1992**, *4*, 425.
(44) Robello, D. R.; Dao, P. T.; Schildkraut, J. S.; Scozzafava, M.; Urankar, E. J.; Willand, C. S. *Chem. Mater.* **1995**, *7*, 284.
(45) Corn, R. M.; Higgins, D. A. *Chem. Rev.* **1994**, *94*, 107.
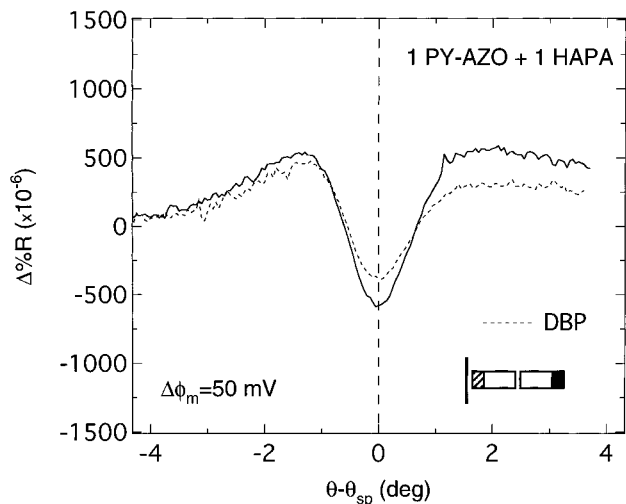(46) Higgins, D. A.; Naujok, R. R.; Corn, R. M. *Chem. Phys. Lett.* **1993**, *213*, 485.

Figure 12. Differential reflectivity ($\Delta\%R$) obtained by EM-SPR measurements for (a) a ZP film with one PY-AZO monolayer and two HAPA monolayers, 1 PY-AZO + 2 HAPA, and (b) a ZP film with two PY-AZO monolayers and one HAPA monolayer, 2 PY-AZO + 1 HAPA. Each of these ZP multilayer films contained a phosphorylated MUD primer layer and a DHP capping monolayer. The curve in (a) has the waveform of a HAPA sample, while (b) has the waveform of a PY-AZO sample. The difference in the waveforms for these two samples is due to the interference between the electrooptical responses of the HAPA and PY-AZO monolayers in the ZP films.

has a waveform similar to the $\Delta\%R$ curve for a single PY-AZO monolayer. The difference in the waveforms for these two samples is due to the interference between the electrooptical responses of the HAPA and PY-AZO monolayers in the ZP films. Figure 13 plots the $\Delta\%R$ curve (solid line) for the 1 PY-AZO + 1 HAPA ZP film and shows a complete cancellation of the electrooptical response of the ZP multilayer. The residual EM-SPR differential reflectivity signal observed from this sample is due to contributions from the metal substrate that have been observed previously.[16] This substrate response is similar to that observed from a four-monolayer centrosymmetric DBP ZP film (which is also plotted in Figure 13 as the dashed line).

These measurements are the first observation of interference effects in EM-SPR measurements on self-assembled noncentrosymmetric films and demonstrate unequivocally that mixed ZP multilayers with differently oriented chromophore monolayers can be created. The amount of interference observed from the mixed ZP multilayers also depends on the electric field profile through

Figure 13. Differential reflectivity ($\Delta\%R$) obtained by EM-SPR measurements for a ZP film with one PY-AZO and one HAPA monolayer, 1 PY-AZO + 1 HAPA (solid line). This ZP multilayer film also contained a phosphorylated MUD primer layer and a DHP capping monolayer. The solid curve shows a complete cancellation of the electrooptical response of the ZP multilayer. The residual EM-SPR differential reflectivity signal observed from this sample is due to contributions from the metal substrate. This substrate response is the same as that observed from a four-monolayer centrosymmetric DBP ZP film (dashed line).

the ultrathin film. For example, a less pronounced interference effect was observed from a 1 HAPA + 1 PY-AZO ZP film as compared to the 1 PY-AZO + 1 HAPA ZP film shown in Figure 13. Differences between these two films are due to the fact that the second ZP monolayer in these samples experiences a slightly lower local electric field strength (as expected from the results of section B), which, in the case of HAPA and PY-AZO, happens to cancel out the slight difference in the magnitude of r_{33} for the two different chromophores.

SUMMARY AND CONCLUSIONS

In this paper, the optical technique of EM-SPR is shown to be an effective method for monitoring the electrostatic field strengths inside ultrathin organic films at electrode surfaces. EM-SPR experiments were used to determine variations in the electric field strength within mixed ZP multilayer films of the nonlinear optical chromophore HAPA and the centrosymmetric molecule DBP. The

changes in electric field strength (ΔE) determined via the modulated EM-SPR reflectivity curves decrease in a linear fashion through the multilayer film. This linear decrease in ΔE is attributed to ion and solvent penetration into the ZP multilayers and implies a quadratic decrease with thickness of the local potential ϕ inside the ZP film. For a 6.7 nm ZP film incorporating one HAPA monolayer, the magnitude of ΔE determined with EM-SPR measurements of 1.4×10^4 V/cm for a $\Delta\phi_m$ of 50 mV (2.8×10^5 V/cm per volt modulation) is consistent with the field strengths calculated by others inside monolayer films at electrode surfaces from electrochromic shifts in fluorescence and electroreflectance measurements.[7,9,10] The EM-SPR technique is a versatile method that should, in the future, provide detailed information on other noncentrosymmetric assemblies on electrode surfaces, including Langmuir−Blodgett films and nonlinear optical polymer films.

The EM-SPR technique is also sensitive to the phase of the complex surface nonlinear susceptibility, and, in a second set of EM-SPR experiments, interference effects between the two nonlinear optical chromophores HAPA and PY-AZO were used to verify directional order in mixed noncentrosymmetric ZP films at electrode surfaces. The differential reflectivity curves from ZP multilayer films composed of different numbers of HAPA and PY-AZO layers exhibit varying degrees of interference, and a complete cancellation of the molecular electrooptical response is observed for a 1 PY-AZO + 1 HAPA ZP multilayer film. These EM-SPR interference effects are similar to those seen in surface SHG experiments and demonstrate that ZP multilayers can be created with multiple noncentrosymmetric monolayers that are oriented in opposite directions. In future studies, we plan to investigate ways of reducing ion and solvent penetration into the ZP films and to examine interference effects within mixed ZP multilayer films as a function of distance between two nonlinear optical chromophore monolayers.